A Sequential Partial Relaxation-Based Technique for Automotive MIMO Radar Imaging

Minh Trinh-Hoang
Rohde und Schwarz GmbH & Co KG
Munich, Germany

Dani Karam
TU Darmstadt
Darmstadt, Germany

Dmytro Rachkov
Sony Europe B.V.
Stuttgart, Germany

Marius Pesavento
TU Darmstadt
Darmstadt, Germany

Abstract—We consider the joint Direction-of-Arrival (DOA), Time-of-Arrival, and Doppler-frequency estimation problem in Multiple-Input-Multiple Output automotive radar systems. To enhance the angular resolution capability, the virtual array concept is employed. For solving the estimation problem we present a multidimensional extension of the recently proposed Partially Relaxed Orthogonal Least Squares Weighted Subspace Fitting (PR-OLS-WSF) algorithm. The PR-OLS-WSF algorithm belongs to the class of computationally efficient greedy algorithms where each source is resolved sequentially. Unlike other greedy algorithms such as the popular Matching Pursuit (MP) and Orthogonal Matching Pursuit (OMP) whose performances are known to severely degrade in both threshold and asymptotic domains, the proposed PR-OLS-WSF algorithm inherits excellent resolution performance from the partial relaxation step involving in the optimization procedure. We show that, based on real measurement data, the proposed algorithm can resolve more targets than the Matching Pursuit algorithm.

Index Terms—MIMO radar, automotive radar, virtual array, sensor array processing, direction-of-arrival estimation, weighted subspace fitting, orthogonal matching pursuit, partial relaxation

I. INTRODUCTION

Multiple-input-multiple-output (MIMO) radar is receiving increasing attention in the automotive radar industry due to the ability to form large virtual array apertures from a relatively small number of transmit and receive antennas [1]. The use of the virtual array concepts requires orthogonal waveforms transmitted from different antennas and therefore comes at the expense of transmitter array gain leading to a reduced Signal-to-Noise ratio (SNR) in the response. However, in automotive radar, the increase of angular resolution capability of the array and the reduction of the required hardware costs are of fundamental importance and justify the loss of array gain [2]. Several multiplexing techniques have been considered for transmission including code division multiplexing (CDM), time division multiplexing (TDM) and frequency division multiplexing (FDM). While CDM is more flexible in the design of the transmission sequences, TDM MIMO radar is attractive as less complex hardware is required. The achievable angular resolution capability of both multiplexing schemes has been investigated in [3] and shown to be fundamentally identical, which favors the use of the simpler TDM technique.

The virtual array concept allows the use of conventional array processing techniques such as conventional beamforming, Capon beamforming [4], ESPRIT [5], MUSIC [6] and orthogonal matching pursuit (OMP) [7], [8]. Recently, the Partial Relaxation (PR) framework has been introduced as a new class of DOA estimators for closely-spaced sources with superior resolution performance similar to Maximum-Likelihood in the threshold domain but with a computational cost comparable to that of spectral subspace methods [9]. Unfortunately, PR techniques lose the performance benefits if the number of sources becomes large. This is attributed to the fact that the manifold relaxation associated with the PR framework is no longer tight. To prevent such performance loss, the PR technique has been incorporated in sequential estimation schemes such as matching pursuit (MP) [10], OMP [7], [8] and Orthogonal Least Squares (OLS) [11], [12]. While the above mentioned sequential estimators are known to be inconsistent for a finite number of antennas the sequential estimators developed under the PR framework show in simulations true super-resolution capability and resolution performance close to the Cramér-Rao Bound [13], [14].

In this paper, we extend the sequential PR estimation framework to the multi-dimensional frequency estimation in MIMO radar setup where the DOA, range and Doppler parameters of multiple targets are jointly estimated. We investigate the resolution performance of the sequential estimation techniques for real MIMO radar data recorded in a measurement campaign at Sony Stuttgart, Germany, and show that the Partially-Relaxed Orthogonal Least Squares Weighted Subspace Fitting (PR-OLS-WSF) method [15] correctly resolves more targets than the classical OLS in the considered scenario.

II. SIGNAL MODEL

We consider a colocated time-division multiplexing (TDM) frequency-modulated continuous-waveform (FMCW) multiple-input-multiple-output (MIMO) radar with M_t transmit and M_r receive antennas [2]. After matched filtering and Discrete Fourier Transformation (DFT) along the fast time dimension and denoting Δf and ΔT_P as the frequency spacing and the time spacing along the fast and slow time dimension, respectively, the virtual array [1], [3] receive signal tensor $\boldsymbol{\mathcal{Y}} \in \mathbb{C}^{K \times M_\mathrm{r} \times M_\mathrm{t} \times L}$ for N point targets is given by

$$\boldsymbol{\mathcal{Y}} = \sum_{n=1}^{N} \beta_n \mathbf{b}(\tau_n) \circ \mathbf{a}_\mathrm{r}(\theta_n) \circ \mathbf{a}_\mathrm{t}(\theta_n) \circ \mathbf{c}(\nu_n) + \boldsymbol{\mathcal{N}} \quad (1)$$

where $\boldsymbol{\beta} = [\beta_1, \ldots, \beta_N]^\mathsf{T}$, $\boldsymbol{\tau} = [\tau_1, \ldots, \tau_N]^\mathsf{T}$, $\boldsymbol{\theta} = [\theta_1, \ldots, \theta_N]^\mathsf{T}$ and $\boldsymbol{\nu} = [\nu_1, \ldots, \nu_P]^\mathsf{T}$ denote the complex amplitudes proportional to the radar cross section (RCS), the path delay for range estimation, the azimuth direction and the Doppler frequency of N targets, respectively. In addition, the vector $\boldsymbol{b}(\tau)$ and $\boldsymbol{c}(\nu)$ are respectively defined as

$$\boldsymbol{b}\left(\tau_n\right) = \left[1, e^{-j2\pi\Delta f\tau_n}, \ldots, e^{-j2\pi(K-1)\Delta f\tau_n}\right]^\mathsf{T} \quad (2a)$$

$$\boldsymbol{c}\left(\nu_n\right) = \left[1, e^{-j2\pi\Delta T_\mathrm{P}\nu_n}, \ldots, e^{-j2\pi(L-1)\Delta T_\mathrm{P}\nu_n}\right]^\mathsf{T} \quad (2b)$$

$\boldsymbol{a}_\mathrm{t}(\theta_n) \in \mathbb{C}^{M_\mathrm{t}}$ and $\boldsymbol{a}_\mathrm{r}(\theta_n) \in \mathbb{C}^{M_\mathrm{r}}$ represent the transmit and receive steering vectors with the m-th and m'-th element denoted by

$$[\boldsymbol{a}_\mathrm{t}(\theta_n)]_m = e^{-j\pi(d_{x,m}^\mathrm{t}\cos\theta_n + d_{y,m}^\mathrm{t}\sin\theta_n)}, \quad (3a)$$

$$[\boldsymbol{a}_\mathrm{r}(\theta_n)]_{m'} = e^{-j\pi(d_{x,m'}^\mathrm{r}\cos\theta_n + d_{y,m'}^\mathrm{r}\sin\theta_n)}, \quad (3b)$$

respectively. The (x,y)-coordinates in (3), i.e., $(d_{x,m}^\mathrm{t}, d_{y,m}^\mathrm{t})$ and $(d_{x,m'}^\mathrm{r}, d_{y,m'}^\mathrm{r})$ denote the locations of the m-th transmit antenna and m'-th receive antenna in half-wavelength, respectively. K defines the number of relevant frequency samples for range estimation, L is the number of slow time samples (i.e. radar pulses), and $\mathcal{N} \in \mathbb{C}^{K \times M_\mathrm{r} \times M_\mathrm{t} \times L}$ denotes the i.i.d. Gaussian measurement noise tensor with power σ^2. After appropriate unfolding the 4D measurement tensor in (1) can be written as

$$\boldsymbol{Y} = (\underbrace{\boldsymbol{C} \odot \boldsymbol{A}_\mathrm{t} \odot \boldsymbol{A}_\mathrm{r}}_{\boldsymbol{H}}) \, \boldsymbol{B}^\mathsf{T} + \boldsymbol{N}, \quad (4)$$

where $\boldsymbol{N}$ is the unfolding of $\mathcal{N}$, $\odot$ denotes the Khatri-Rao (column-wise Kronecker) product,

$$\boldsymbol{B} = [\beta_1\mathbf{b}(\tau_1), \ldots, \beta_n\mathbf{b}(\tau_N)] \in \mathbb{C}^{K \times N} \quad (5)$$

$$\boldsymbol{C} = [\mathbf{c}(\nu_1), \ldots, \mathbf{c}(\nu_N)] \in \mathbb{C}^{L \times N} \quad (6)$$

$$\boldsymbol{A} = [\boldsymbol{a}(\theta_1), \ldots, \boldsymbol{a}(\theta_N)] = \boldsymbol{A}_\mathrm{t} \odot \boldsymbol{A}_\mathrm{r} \in \mathbb{C}^{M \times N} \quad (7)$$

$$\boldsymbol{H} = [\boldsymbol{h}(\theta_1, \nu_1), \ldots, \boldsymbol{h}(\theta_N, \nu_N)] = \boldsymbol{C} \odot \boldsymbol{A} \in \mathbb{C}^{LM \times N} \quad (8)$$

with $M = M_\mathrm{t}M_\mathrm{r}$ denoting the number of antennas in the virtual array and

$$\boldsymbol{A}_\mathrm{t} = [\boldsymbol{a}_\mathrm{t}(\theta_1), \ldots, \boldsymbol{a}_\mathrm{t}(\theta_N)] \in \mathbb{C}^{M_\mathrm{t} \times N} \quad (9a)$$

$$\boldsymbol{A}_\mathrm{r} = [\boldsymbol{a}_\mathrm{r}(\theta_1), \ldots, \boldsymbol{a}_\mathrm{r}(\theta_N)] \in \mathbb{C}^{M_\mathrm{r} \times N}. \quad (9b)$$

Given the unfolded measurement model (4) we consider the range frequency samples as independent measurements and compute the sample covariance matrix as

$$\hat{\boldsymbol{R}} = \frac{1}{K}\boldsymbol{Y}\boldsymbol{Y}^\mathsf{H} = \hat{\boldsymbol{U}}\hat{\boldsymbol{\Lambda}}\hat{\boldsymbol{U}}^\mathsf{H} = \hat{\boldsymbol{U}}_\mathrm{s}\hat{\boldsymbol{\Lambda}}_\mathrm{s}\hat{\boldsymbol{U}}_\mathrm{s}^\mathsf{H} + \hat{\boldsymbol{U}}_\mathrm{n}\hat{\boldsymbol{\Lambda}}_\mathrm{n}\hat{\boldsymbol{U}}_\mathrm{n}^\mathsf{H} \quad (10)$$

where $\hat{\boldsymbol{U}}_\mathrm{s} \in \mathbb{C}^{LM \times N}$ refers to the signal subspace matrix containing the N-principal eigenvectors of $\hat{\boldsymbol{R}}$ and $\hat{\boldsymbol{\Lambda}}_\mathrm{s} \in \mathbb{C}^{N \times N}$ is the diagonal matrix comprising the associated N-largest eigenvalues $\lambda_1 \geq \lambda_2, \ldots, \geq \lambda_N$. Similarly, $\hat{\boldsymbol{U}}_\mathrm{n} \in \mathbb{C}^{LM \times (LM-N)}$ refers to the noise subspace matrix containing the $(LM - N)$ minor noise eigenvectors with corresponding eigenvalues $\lambda_{N+1} \geq \lambda_{N+2} \geq \ldots \geq \lambda_{LM}$ on the main diagonal of $\hat{\boldsymbol{\Lambda}}_\mathrm{n} \in \mathbb{C}^{(LM-N) \times (LM-N)}$.

We remark that in the ideal noise free case and for a sufficiently large number of frequency samples $K \geq N$ the signal subspace matrix and the Doppler-DoA steering matrix span the same signal subspace, hence $\mathcal{R}(\boldsymbol{H}) = \mathcal{R}(\hat{\boldsymbol{U}}_\mathrm{s})$.

III. THE PARTIAL RELAXATION ORTHOGONAL LEAST SQUARES WEIGHTED SUBSPACE FITTING ALGORITHM

A. Motivation and Derivation

In this section, the concept of the PR-OLS-WSF estimator derived in [15] is explained and applied in the context of MIMO radar. By relaxing the range frequency samples as independent measurements, the formulation of the conventional Deterministic Maximum Likelihood (DML) for estimating the azimuth angles $\boldsymbol{\theta}$ and the Doppler frequencies $\boldsymbol{\nu}$ is given by

$$\left\{\hat{\boldsymbol{\theta}}, \hat{\boldsymbol{\nu}}\right\} = \underset{\boldsymbol{\theta}, \boldsymbol{\nu}, \boldsymbol{B}^\mathsf{T}}{\arg\min} \left\|\boldsymbol{Y} - \boldsymbol{H}(\boldsymbol{\theta}, \boldsymbol{\nu})\boldsymbol{B}^\mathsf{T}\right\|_\mathsf{F}. \quad (11)$$

As the optimization problem in (11) is nonconvex with multiple local minima, finding the optimal solutions of the azimuth angles and the Doppler frequencies jointly for $N > 2$ targets is not computationally tractable. To reduce the computational complexity, the OLS technique in [11] was developed. Instead of jointly estimating the azimuth angles and Doppler frequencies of N targets in one optimization problem, the OLS technique sequentially estimates the azimuth angle and the Doppler frequency of only one target in each iteration. More precisely, given the previously estimated azimuth angles $\hat{\boldsymbol{\theta}}^{(k-1)}$ and Doppler frequencies $\hat{\boldsymbol{\nu}}^{(k-1)}$, the optimization problem in the k-th iteration for $k = 1, \ldots, N$ is given by

$$\left\{\hat{\theta}^{(k)}, \hat{\nu}^{(k)}\right\} = \underset{\theta, \nu, \boldsymbol{B}^{(k)\mathsf{T}}}{\arg\min} \left\|\boldsymbol{Y} - \left[\hat{\boldsymbol{H}}^{(k-1)}, \boldsymbol{h}(\theta, \nu)\right]\boldsymbol{B}^{(k)\mathsf{T}}\right\|_\mathsf{F}^2$$

$$= \underset{\theta, \nu}{\arg\min} \ \mathrm{tr}\left\{\boldsymbol{P}_{\left[\hat{\boldsymbol{H}}^{(k-1)}, \boldsymbol{h}(\theta, \nu)\right]}^\perp \hat{\boldsymbol{R}}\right\},$$

$$(12)$$

where $\hat{\boldsymbol{H}}^{(k-1)} = \boldsymbol{H}(\hat{\boldsymbol{\theta}}^{(k-1)}, \hat{\boldsymbol{\nu}}^{(k-1)})$ and $\boldsymbol{P}_{\boldsymbol{A}}^\perp = \boldsymbol{I} - \boldsymbol{A}(\boldsymbol{A}^\mathsf{H}\boldsymbol{A})^{-1}\boldsymbol{A}^\mathsf{H}$ is the projection matrix onto the subspace that is the orthogonal complement to the subspace span$(\boldsymbol{A})$. Then the estimated azimuth angle and Doppler frequency set in each iteration $k = 1, \ldots, N$ is correspondingly updated as

$$\Omega^{(k)} = \Omega^{(k-1)} \cup \left\{\left(\hat{\theta}^{(k)}, \hat{\nu}^{(k)}\right)\right\}. \quad (13)$$

After the azimuth angle and the Doppler frequency of the k-th target are resolved, the complex amplitude $\hat{\beta}^{(k)}$ and the $\hat{\tau}^{(k)}$ is estimated as

$$\left\{\hat{\beta}^{(k)}, \hat{\tau}^{(k)}\right\} = \underset{\beta, \tau}{\arg\min} \left\|\boldsymbol{Y} - \beta\boldsymbol{h}\left(\hat{\theta}^{(k)}, \hat{\nu}^{(k)}\right)\boldsymbol{b}(\tau)^\mathsf{T}\right\|_\mathsf{F}^2,$$

or equivalently, if only the path delay $\hat{\tau}^{(k)}$ is of interest (14)

$$\hat{\tau}^{(k)} = \underset{\tau}{\arg\max} \left|\boldsymbol{h}\left(\hat{\theta}^{(k)}, \hat{\nu}^{(k)}\right)^\mathsf{H}\boldsymbol{Y}\boldsymbol{b}(\tau)^\star\right|^2, \quad (15)$$

where $(\cdot)^\star$ denotes the conjugate operator. Compared with the DML estimator, the computational cost of the OLS technique is drastically reduced as each target is resolved sequentially in each iteration. Nevertheless, the drawback of the OLS technique is the limited resolution capability, similarly to the conventional beamformer or the FFT method.

In order to improve the estimation performance of the OLS algorithm while keeping the computational cost low,

the PR-OLS-WSF in [15] was derived. In the PR-OLS-WSF algorithm, two major changes to the classical OLS technique are adopted. First, instead of approximately solving the DML optimization problem, the PR-OLS-WSF algorithm attempts to solve the Weighted Subspace Fitting (WSF) [16] optimization problem, in which the unfolded receive tensor $\boldsymbol{Y}$ is replaced by the weighted subspace matrix $\hat{\boldsymbol{U}}_s \boldsymbol{W}^{1/2}$ with $\boldsymbol{W} = \left(\hat{\boldsymbol{\Lambda}}_s - \hat{\sigma}_n^2 \boldsymbol{I}_N\right)^2 \hat{\boldsymbol{\Lambda}}_s^{-1}$ with $\hat{\sigma}_n^2 = \frac{1}{M-N} \sum_{k=N+1}^{M} \hat{\lambda}_k$. This choice on the matching term simultaneously improves the asymptotic estimation performance [16] as well as reduces the computational cost of the associated PR-OLS-WSF algorithm. More details on the efficient implementation of the PR-OLS-WSF algorithm will be explained in the next subsection. Second, compared to the OLS technique which only accounts for the $(k-1)$-previously estimated targets while estimating the parameters of the k-th target, the PR-OLS-WSF algorithm considers the $(N - k)$ remaining targets. However, instead of enforcing structure on the $(N - k)$ remaining signals, the structure is relaxed to some arbitrary matrix $\boldsymbol{G}^{(k)} \in \mathbb{C}^{LM \times (N-k)}$. Hence, in the k-th iteration, the matrix $\boldsymbol{H}(\theta, \nu)$ in (11) is separated into the relaxed part $\boldsymbol{G}^{(k)}$ and $\boldsymbol{H}^{(k)}(\theta, \nu) = [\hat{\boldsymbol{H}}^{(k-1)}, \boldsymbol{h}(\theta, \nu)]$ where $\hat{\boldsymbol{H}}^{(k-1)}$ contains the $(k-1)$-previously estimated DOAs and Doppler frequencies. Similarly, the nuisance parameter is separated into the part that belongs to the structured signal part, namely $\boldsymbol{F}^{(k)} \in \mathbb{C}^{k \times N}$, and $\boldsymbol{E}^{(k)} \in \mathbb{C}^{(N-k) \times N}$ which belongs to the unstructured signal part $\boldsymbol{G}^{(k)}$. In essence, the optimization problem in the k-th iteration is given by [15, Eqs. (13)-(16)]

$$
\begin{aligned}
\left\{\hat{\theta}^{(k)}, \hat{\nu}^{(k)}\right\} &= \underset{\theta, \nu}{\arg\min} \ \underset{\boldsymbol{F}^{(k)}, \boldsymbol{G}^{(k)}, \boldsymbol{E}^{(k)}}{\min} \\
&\left\| \hat{\boldsymbol{U}}_s \boldsymbol{W}^{1/2} - \left[\hat{\boldsymbol{H}}^{(k-1)}, \boldsymbol{h}(\theta, \nu) \right] \boldsymbol{F}^{(k)} - \boldsymbol{G}^{(k)} \boldsymbol{E}^{(k)} \right\|_{\mathsf{F}}^2 \\
&= \sum_{q=N-k+1}^{N} \lambda_q \left(\boldsymbol{P}^{\perp}_{\left[\hat{\boldsymbol{H}}^{(k-1)}, \boldsymbol{h}(\theta, \nu)\right]} \hat{\boldsymbol{U}}_s \boldsymbol{W} \hat{\boldsymbol{U}}_s^{\mathsf{H}} \right).
\end{aligned}
\tag{16}
$$

The PR-OLS-WSF DOA estimation technique is summarized in Algorithm 1. We remark that the main computational complexity of the PR-OLS-WSF algorithm lies mostly in Step 3, Equation 16, where the eigenvalue decomposition of a matrix of size $LM \times LM$ is required for all possible azimuth angles and Doppler frequencies. In the following, an efficient implementation of the PR-OLS-WSF algorithm is outline, which simplifies the aforementioned expensive spectral search.

B. Efficient Implementation

A key idea in reducing the computational complexity of the PR-OLS-WSF algorithm. Instead of performing the full eigenvalue decomposition on a $LM \times LM$ matrix as in (16), we compute only a subset of k smallest eigenvalues of an $N \times N$ matrix by rewriting the concentrated cost function in (16) as follows

$$
\begin{aligned}
&\sum_{q=N-k+1}^{N} \lambda_q \left(\boldsymbol{P}^{\perp}_{[\hat{\boldsymbol{H}}^{(k-1)}, \boldsymbol{h}(\theta, \nu)]} \hat{\boldsymbol{U}}_s \boldsymbol{W} \hat{\boldsymbol{U}}_s^{\mathsf{H}} \right) \\
&= \sum_{q=N-k+1}^{N} \lambda_q \left(\boldsymbol{W}^{1/2} \hat{\boldsymbol{U}}_s^{\mathsf{H}} \boldsymbol{P}^{\perp}_{[\hat{\boldsymbol{H}}^{(k-1)}, \boldsymbol{h}(\theta, \nu)]} \hat{\boldsymbol{U}}_s \boldsymbol{W}^{1/2} \right) \\
&= \sum_{q=N-k+1}^{N} \lambda_q \left(\boldsymbol{M}^{(k-1)} - \tilde{\boldsymbol{z}}(\theta, \nu)^{(k-1)} \tilde{\boldsymbol{z}}(\theta, \nu)^{(k-1)\mathsf{H}} \right),
\end{aligned}
\tag{17}
$$

with the $N \times N$ matrix $\boldsymbol{M}^{(k-1)} = \boldsymbol{W}^{1/2} \hat{\boldsymbol{U}}_s^{\mathsf{H}} \boldsymbol{P}^{\perp}_{\hat{\boldsymbol{H}}^{(k-1)}} \hat{\boldsymbol{U}}_s \boldsymbol{W}^{1/2}$ and the vector $\tilde{\boldsymbol{z}}_\ell^{(k-1)} = \boldsymbol{W}^{1/2} \hat{\boldsymbol{U}}_s^{\mathsf{H}} \frac{\boldsymbol{P}^{\perp}_{\boldsymbol{H}^{(k-1)}} \boldsymbol{h}(\theta, \nu)}{\| \boldsymbol{P}^{\perp}_{\boldsymbol{H}^{(k-1)}} \boldsymbol{h}(\theta, \nu) \|}$. For faster computation of the vector $\tilde{\boldsymbol{z}}_\ell^{(k-1)}$, the Gram-Schmidt process is applied to orthonormalize the matrix $\hat{\boldsymbol{H}}^{(k-1)}$ in each iteration after the parameters of one target are estimated. In addition, if the matrix $\boldsymbol{M}^{(k-1)}$ admits the eigenvalue decomposition $\boldsymbol{M}^{(k-1)} = \boldsymbol{V}^{(k-1)} \boldsymbol{W}^{(k-1)} \boldsymbol{V}^{(k-1)\,\mathsf{H}}$, then the cost function in (17) is expressed as

$$
\begin{aligned}
&\sum_{q=N-k+1}^{N} \lambda_q \left(\boldsymbol{M}^{(k-1)} - \tilde{\boldsymbol{z}}(\theta, \nu)^{(k-1)} \tilde{\boldsymbol{z}}(\theta, \nu)^{(k-1)\mathsf{H}} \right) \\
&= \sum_{q=N-k+1}^{N} \lambda_q \left(\boldsymbol{W}^{(k-1)} - \boldsymbol{z}(\theta, \nu)^{(k-1)} \boldsymbol{z}(\theta, \nu)^{(k-1)\mathsf{H}} \right),
\end{aligned}
\tag{18}
$$

with $\boldsymbol{z}(\theta, \nu)^{(k-1)} = \boldsymbol{V}^{(k-1)\mathsf{H}} \tilde{\boldsymbol{z}}(\theta, \nu)^{(k-1)}$. The eigenvalues of the rank-one modified Hermitian matrix in (18) can efficiently be computed using the iterative method in [17] (also refer to [9, Th. 1]). Along the same line, the updates for $\boldsymbol{V}^{(k)}$ and $\boldsymbol{W}^{(k)}$ can be efficiently computed by adopting the same iterative procedure. If the mixing vectors $\boldsymbol{h}(\theta, \nu)$ for all possible candidates azimuth angle θ and the Doppler frequency ν are precomputed and collected in the dictionary matrix $\bar{\boldsymbol{H}}$, then the computationally efficient implementation of the PR-OLS-WSF method is summarized in Algorithm 2.

IV. EXPERIMENTAL RESULTS WITH MIMO RADAR

In this section, we evaluate the performance of our algorithm using real MIMO radar data recorded in a measurement campaign at Sony Stuttgart. $M_t = 3$ transmit antennas send a TDM signal, which is then collected by a Uniform Linear Array (ULA) of $M_r = 4$ receive antennas with a spacing

---

Algorithm 1 PR-OLS-WSF Algorithm

1: **Initialization:** Iteration index $k = 0$, initial jointly estimated DOA and Doppler frequency set $\Omega^{(0)} = \emptyset$ and initial empty mixing matrix $\hat{\boldsymbol{H}}^{(0)} = []$

2: **for** $k = 1, \ldots, N$ **do**

3:     Find the azimuth angle and the Doppler frequency $\left\{\hat{\theta}^{(k)}, \hat{\nu}^{(k)}\right\}$ of the k-th target according to (16).

4:     Estimate the delay $\hat{\tau}^{(k)}$ of the k-th target as in (15)

5:     Update the estimated parameter set and the corresponding estimated mixing matrix
$$
\Omega^{(k)} = \Omega^{(k-1)} \cup \left\{ \left(\hat{\theta}^{(k)}, \hat{\nu}^{(k)}\right) \right\},
$$
$$
\hat{\boldsymbol{H}}^{(k)} = \left[\hat{\boldsymbol{H}}^{(k-1)}, \boldsymbol{h}\left(\hat{\theta}^{(k)}, \hat{\nu}^{(k)}\right) \right].
$$

6: **end for**

7: **return** The estimated parameters $\hat{\theta}^{(k)}, \hat{\nu}^{(k)}$ and $\hat{\tau}^{(k)}$ for $k = 1, \ldots, N$ of the N targets.

Algorithm 2 Efficient Implementation of the PR-OLS-WSF Algorithm

1: **Initialization:** Iteration index $k = 0$, initial diagonalizing matrix $\boldsymbol{V}^{(0)} = \boldsymbol{I}_N$, initial weighting matrix $\boldsymbol{W}^{(0)} = \boldsymbol{W}$, initial normalized dictionary $\bar{\boldsymbol{H}}^{(0)} = \bar{\boldsymbol{H}} = \left[\bar{\boldsymbol{h}}_1^{(0)}, \ldots, \bar{\boldsymbol{h}}_G^{(0)} \right]$ (such that each column is unit-norm)

2: **for** $k = 1, \ldots, N$ **do**

3: Find the index p such that
$$p = \underset{g=1,\ldots,G}{\arg\min} \sum_{q=N-k+1}^{N} \lambda_q \left(\boldsymbol{W}^{(k-1)} - \boldsymbol{z}_g \boldsymbol{z}_g^{\mathsf{H}} \right)$$
using the rank-one modification problem in [9, Theorem 1] (also see [17]) with $\boldsymbol{z}_g = \boldsymbol{V}^{(k-1)\,\mathsf{H}} \tilde{\boldsymbol{U}}_s^{\mathsf{H}} \bar{\boldsymbol{h}}_g^{(k-1)}$ and $\tilde{\boldsymbol{U}}_s = \hat{\boldsymbol{U}}_s \boldsymbol{W}^{1/2}$. The optimal index p corresponds to the estimated azimuth angle $\hat{\theta}^{(k)}$ and Doppler frequency $\hat{\nu}^{(k)}$.

4: Compute the diagonalizing matrix $\boldsymbol{V}_{\mathrm{mod}}^{(k)}$ and the diagonal matrix $\boldsymbol{W}^{(k)}$ using the rank-one modification problem
$$\boldsymbol{V}_{\mathrm{mod}}^{(k)} \boldsymbol{W}^{(k)} \boldsymbol{V}_{\mathrm{mod}}^{(k)\mathsf{H}} = \boldsymbol{W}^{(k-1)} - \boldsymbol{V}^{(k-1)\mathsf{H}} \tilde{\boldsymbol{U}}_s^{\mathsf{H}} \bar{\boldsymbol{h}}_p^{(k-1)} \bar{\boldsymbol{h}}_p^{(k-1)\mathsf{H}} \tilde{\boldsymbol{U}}_s \boldsymbol{V}^{(k-1)}$$

5: Update the orthogonal basis $\boldsymbol{V}^{(k)}$ and the updated dictionary matrix $\bar{\boldsymbol{H}}^{(k)} = \left[\bar{\boldsymbol{h}}_1^{(k)}, \ldots, \bar{\boldsymbol{h}}_G^{(k)} \right]$ as follows
$$\bar{\boldsymbol{H}}^{(k)} = \bar{\boldsymbol{H}}^{(k-1)} - \frac{1}{\|\bar{\boldsymbol{h}}_p^{(k-1)}\|_2^2} \bar{\boldsymbol{h}}_p^{(k-1)} \bar{\boldsymbol{h}}_p^{(k-1)\mathsf{H}} \bar{\boldsymbol{H}}^{(k-1)}.$$

6: Normalize the updated dictionary matrix $\bar{\boldsymbol{H}}^{(k)}$ columnwise.

7: Estimate the delay $\hat{\tau}^{(k)}$ of the k-th target based on $\hat{\theta}^{(k)}$ and $\hat{\nu}^{(k)}$ according to (15)

8: **end for**

9: **return** The estimated parameters $\hat{\theta}^{(k)}$, $\hat{\nu}^{(k)}$ and $\hat{\tau}^{(k)}$ for $k = 1, \ldots, N$ of the N targets.

---

equal to half-wavelength $(d = \lambda/2)$. The antenna setup is illustrated in Fig. 1 where also the corresponding virtual array is displayed. The measurement consists of 901 frames. Each
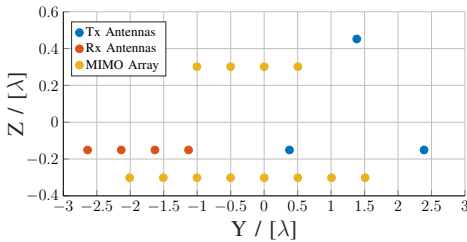

Fig. 1: MIMO Array Structure

frame contains the measured signal which is reshaped into a three-dimensional Radar Data Cube (RDC) of dimension $(K \times M \times L)$ as depicted in Table I.

In this scenario, a radar-vehicle navigates in a parking lot with stationary cars. The main goal is also to achieve a detection

TABLE I: Radar Data Cube Specifications

Notation	Explanation	Value
K	Fast time samples	512
$M = M_{\mathrm{t}} \times M_{\mathrm{r}}$	Number of virtual array elements	12
L	Number of Pulses/Slow time samples	128

and accurate estimation of the distance, relative angle and velocity corresponding to cars in front of a moving radar-vehicle. Note that the radar sensor is placed at the front right corner of the radar-vehicle and is oriented to sense the scene forward in the driving direction. There is no other object moving in the scene except for the radar-vehicle. Thus, all velocities estimated hereinafter represent the Doppler velocity of the radar-vehicle with respect to the detected stationary objects. Moreover, all detection and estimation results are visualized in the local coordinate system of the radar sensor as in Fig. 3 and Fig. 5. In order to provide a reference representation of the scene driven, visual information is recorded by a camera sensor placed at the middle front of the radar-vehicle as in Fig. 2 and Fig. 4. We compare the performance of the proposed method, i.e., PR-OLS-WSF to the Matching Pursuit (MP) algorithm, where the parameters are sequentially estimated using multidimensional FFT.
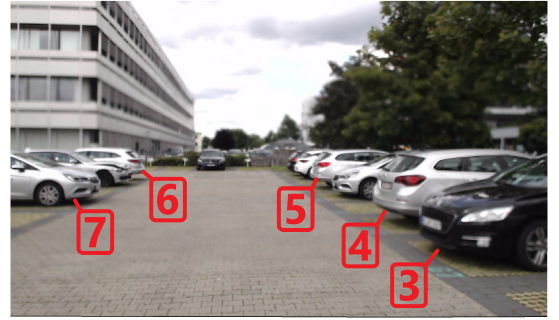

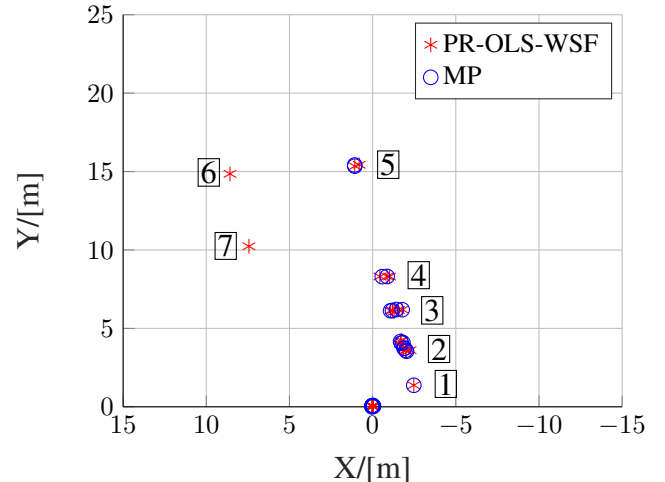Fig. 2: Camera image of frame 194 at $t = 6.43$s

Fig. 3: Estimation result of frame 194

Fig. 2 and Fig. 4 provide camera images of the frames

194 and 234, respectively. The detected targets obtained via both proposed algorithms are also visualized in the local coordinate system of the radar sensor, see Fig. 3 and Fig. 5. For easier illustration, the targets are numbered according to the respective camera image.

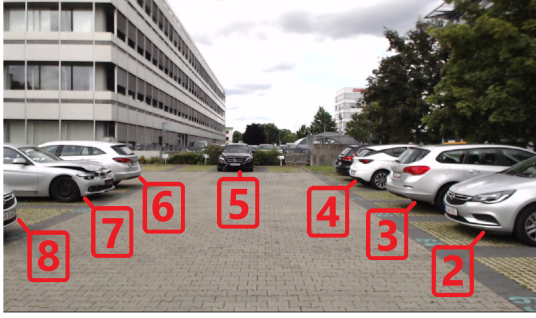The PR-OLS-WSF algorithm takes into account not only the

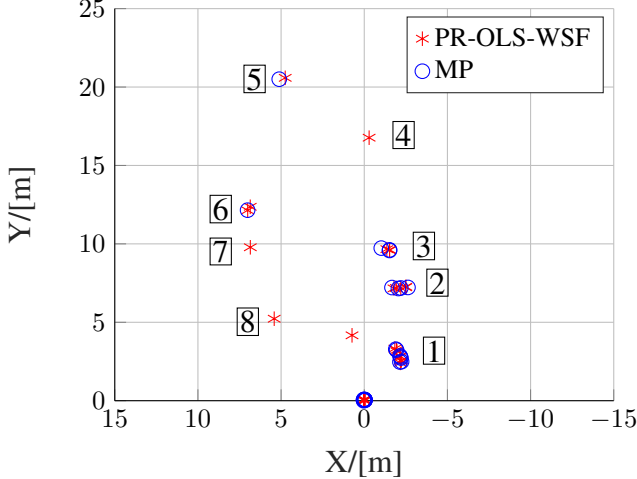Fig. 4: Camera image of frame 234 at $t = 7.77$s

Fig. 5: Estimation result of frame 234

impact of previously estimated source, like the case of MP, but also any potential contribution from remaining $(N - k)$ sources in each iteration. This remark explains the improved performance of PR-OLS-WSF, which is illustrated in Fig. 3 and Fig. 5 . In Fig. 3, the PR-OLS-WSF algorithm is able to detect two more targets than the MP algorithm. Similarly, in Fig. 5 , PR-OLS-WSF can detect three more targets than MP. This suggests that PR-OLS-WSF is a promising estimators in applications where the accurate detection is crucial.

Nevertheless, the drawback of the PR-OLS-WSF algorithm is higher execution time compared to the MP algorithm. Despite the acceleration procedure introduced in Algorithm 2, computation of specific eigenvalues is required in the PR-OLS-WSF algorithm as in (3). More precisely, in each iteration, the azimuth angle and Doppler frequency of one particular target is estimated by computing a two-dimensional spectrum and then searching for the minimum. The delay is then estimated by a one-dimensional grid search. Furthermore,

each iteration requires additional computation to update the dictionary matrix $\bar{\boldsymbol{H}}^{(k)}$ based on the current estimation. On the contrary, the MP algorithm only requires the computation of a 3D FFT-based in each estimation to estimate the path delay, angle and Doppler frequency simultaneously.

V. Conclusions

In this paper, we extend the PR-OLS-WSF algorithm of [15] to the 3D-harmonic estimation problem in synthetic MIMO radar. We provide a fast implementation based on eigendecompositions of rank-one modifications of diagonal matrices that can be efficiently computed using the rational function approximation algorithm [17], [9]. Experimental results with real MIMO radar measurements reveal superior resolution capability of the proposed algorithm compared to classical Matching Pursuit.

References

[1] J. Li and P. Stoica, "MIMO Radar with Colocated Antennas," *IEEE Signal Processing Magazine*, vol. 24, no. 5, pp. 106–114, Sep. 2007.

[2] S. Sun, A. P. Petropulu, and H. V. Poor, "MIMO Radar for Advanced Driver-Assistance Systems and Autonomous Driving: Advantages and Challenges," *IEEE Signal Processing Magazine*, vol. 37, no. 4, pp. 98–117, Jul. 2020.

[3] K. Rambach and Bin Yang, "MIMO radar: time division multiplexing vs. code division multiplexing," in *Int. Conf. on Radar Sys. (Radar 2017)*. Belfast, UK: Institution of Engineering and Technology, 2017.

[4] J. Capon, "High-resolution frequency-wavenumber spectrum analysis," *Proceedings of the IEEE*, vol. 57, no. 8, pp. 1408–1418, 1969.

[5] R. Roy and T. Kailath, "ESPRIT-Estimation of Signal Parameters via Rotational Invariance Techniques," *IEEE Trans. Signal Process.*, vol. 37, no. 7, pp. 984–995, 1989.

[6] R. Schmidt, "Multiple emitter location and signal parameter estimation," *IEEE Trans. Antennas Propag.*, vol. 34, no. 3, pp. 276–280, 1986.

[7] J. Tropp, A. Gilbert, and M. Strauss, "Simultaneous sparse approximation via greedy pursuit," in *Proc. IEEE Int. Conf. on Acoust., Speech, Signal Process. (ICASSP)*, vol. 5, 2005, pp. 721–724.

[8] J. A. Tropp, A. C. Gilbert, and M. J. Strauss, "Algorithms for simultaneous sparse approximation. Part I: Greedy pursuit," *Signal Processing*, vol. 86, no. 3, pp. 572–588, Mar. 2006.

[9] M. Trinh-Hoang, M. Viberg, and M. Pesavento, "Partial Relaxation Approach: An Eigenvalue-Based DOA Estimator Framework," *IEEE Trans. Signal Process.*, vol. 66, no. 23, pp. 6190–6203, 2018.

[10] S. Mallat and Z. Zhang, "Matching pursuits with time-frequency dictionaries," *IEEE Trans. Signal Process.*, vol. 41, no. 12, pp. 3397–3415, Dec. 1993.

[11] S. Chen, S. A. Billings, and W. Luo, "Orthogonal Least Squares Methods and Their Application to Non-linear System Identification," *International Journal of Control*, vol. 50, no. 5, pp. 1873–1896, 1989.

[12] I. Ziskind and M. Wax, "Maximum likelihood localization of multiple sources by alternating projection," *IEEE Trans. Acoust., Speech, and Signal Process.*, vol. 36, no. 10, pp. 1553–1560, Oct. 1988.

[13] M. Pesavento, M. Trinh-Hoang, and M. Viberg, "Three more Decades in Array Signal Processing Research: An Optimization and Structure Exploitation Perspective," Oct. 2022, arXiv:2210.15012 [eess].

[14] M. Trinh-Hoang, W.-K. Ma, and M. Pesavento, "A partial relaxation DOA estimator based on orthogonal matching pursuit," in *Proc. IEEE Int. Conf. on Acoust., Speech, Signal Process. (ICASSP)*, May 2020, pp. 4806–4810.

[15] D. Schenck, K. Lübbe, M. Trinh-Hoang, and M. Pesavento, "Partially relaxed orthogonal least squares weighted subspace fitting direction-of-arrival estimation," in *IEEE International Conference on Acoustics, Speech and Signal Processing (ICASSP)*, May 2022, pp. 5028–5032.

[16] M. Viberg and B. Ottersten, "Sensor Array Processing based on Subspace Fitting," *IEEE Trans. Signal Process.*, vol. 39, no. 5, pp. 1110–1121, 1991.

[17] J. R. Bunch, C. P. Nielsen, and D. C. Sorensen, "Rank-One Modification of the Symmetric Eigenproblem," *Numerische Mathematik*, vol. 31, no. 1, pp. 31–48, 1978.